Structure and Compositional Changes of Eucalyptus Fiber after Various Cycles of Continuous Screw Extrusion Steam Explosion

Yan-Hong Feng,[a] Hui-Ting Zhong,[a] Yong Liang,[a] Bo Lei,[a] Hong Chen,[a] Xiao-Chun Yin,[a]* and Xing-Xing Yu [b,]**

A continuous screw extrusion steam explosion (SESE) pretreatment method was used to disrupt the structure of eucalyptus fiber. The effects of increasing numbers of SESE pretreatment cycles on the structure and composition of eucalyptus fiber were investigated. Lignin was isolated from the eucalyptus fiber *via* the phosphoric acid method under modest reaction conditions (50 °C), and was characterized. The SESE pretreatment led to a decrease in crystallinity and degraded the hemicellulose and cellulose. The surface of the eucalyptus fiber was damaged by SESE pretreatment, and significant surface debris were observed. The isolated lignin was typical of guaiacyl-syringyl (G-S)-enriched lignin of eucalyptus hardwood. The SESE pretreatment led to the cleavage of ether linkages and condensation of lignin, and thus a more heterogeneous structure compared with that of raw lignin. The increased molecular weight of SESE-pretreated lignin showed that condensation was more pronounced with increased numbers of SESE cycles. The thermostability of lignin increased after three SESE cycles and remained stable with further cycles. This corresponded to the trend in the molecular weight of lignin with increased SESE pretreatment. The SESE pretreatment was more efficient for pretreating eucalyptus fiber than conventional batch-type steam explosion, and thus is more suitable for industrial application.

Keywords: Continuous screw extrusion steam explosion; Eucalyptus; Lignin; Structure; Chemical composition

Contact information: a: National Engineering Research Center of Novel Equipment for Polymer Processing, The Key Laboratory of Polymer Processing Engineering of the Ministry of Education, South China University of Technology, Guangzhou 510641, P.R. China; b: Kingfa Science and Technology Co., Ltd., Guangzhou 510663, P. R. China;
*Corresponding authors: * xcyin@scut.edu.cn; ** yuxingxing@kingfa.com.cn*

INTRODUCTION

Lignocellulosic biomass is a sustainable and renewable source for value-added biochemicals, biofuels, and composites. Lignocellulosic biomass consists of three major biopolymers, namely cellulose, hemicellulose, and lignin, each of which has a complex structure (Pu *et al.* 2013). The industrial utilization of lignocellulosic biomass has been impeded by the innate close association of these three components. Pretreatment processes are therefore useful for disrupting the structure and inner links of lignocellulosic material (Meng and Ragauskas 2014). The purpose of a pretreatment is to alter or remove the physical and chemical impediments that inhibit access by enzymes and chemical reagents to the biomass. Many pretreatment approaches have been developed, including hot water, dilute acid, ammonia fiber expansion, and aqueous ammonia pretreatments. The main

applications of pretreated lignocellulose materials are in biorefining, functional materials, and reinforcing materials (Karimi and Taherzadeh 2016). Among the various pretreatment methods, the steam explosion (SE) method is an environmentally friendly and relatively low-cost process that does not use chemicals. Subjecting lignocellulosic material to pressurized steam for a certain amount of time followed by sudden decompression results in the disruption of its structure (Zhao *et al.* 2012). When the temperature reaches 200 °C, hemicellulose acetyl groups and water form an acidic environment that promotes the degradation of lignin and hemicellulose (Inoue *et al.* 2008). Disruption of the physical structure and the degradation of lignin and hemicellulose increase the accessibility of the remaining cellulose. The SE method has traditionally been performed using a batch kettle, which is not industrially viable. A continuous pretreatment system is necessary for industrial application.

The continuous SE of lignocellulosic materials has been recently reported. However, reported continuous SE methods typically require heating systems and steam generators, and have experienced significant steam loss during decompression and severe abrasion of the blow valve (Zimbardi *et al.* 1999; Fang *et al.* 2011b). These deficiencies limit the large-scale pretreatment of lignocellulosic materials (Fang *et al.* 2011a,b). A screw extrusion steam explosion (SESE) method has been developed based on screw extrusion in the polymer molding and food industries (Feng *et al.* 2016; Ma *et al.* 2016). The authors previously reported a continuous SESE process that had a high production capacity. The SESE pretreatment method was developed to realize continuous production for industrial application. In traditional steam explosion, lignocellulosic material is subjected to pressurized steam, and subsequent decompression results in disruption of its structure. The SESE apparatus features a specially designed screw system. The high shearing force and friction between the material, screw, and barrel disrupts the tissue structure of the lignocellulosic material, and it also heats the material. In this study, eucalyptus was pretreated by the SESE method to determine whether SESE pretreatment is suitable for hardwood and to determine how SESE pretreatment affects hardwood. These findings on the SESE pretreatment of eucalyptus could potentially expand the application of SESE in enzymatic hydrolysis and biocomposites. The pretreatment intensity can be readily controlled by adjusting the number of SESE pretreatment cycles. Compared to batch-type steam explosion, SESE has lower energy requirements and it allows for continuous production, making it more suitable for industrial application. The SESE pretreatment described in this study represents a continuous high-efficiency pretreatment process that dramatically decreases the eucalyptus fiber size. This pretreatment could potentially be used to improve the accessibility during enzymatic hydrolysis and increase the interfacial contact area between eucalyptus fiber and plastics.

Lignin is a heterogeneous and highly cross-linked macromolecule, and its structure can change dramatically during SESE. To probe the effects of SESE on lignin, a separation method that yields lignin and that is more representative of the lignin present in the eucalyptus is required. Zhang *et al*. (2007) reported a method to separate lignin using phosphoric acid. In contrast to alkaline cooking and traditional organic solvent methods, the phosphoric acid separation method is conducted at temperatures < 50 °C, which minimizes inhibitor production and lignin modification that often occurs at higher temperatures. The degree of modification of the lignin isolated using the phosphoric acid method was the lowest amongst the reported separation methods, as evidenced by Fourier-transform infrared (FTIR) and ^{13}C nuclear magnetic resonance (^{13}C NMR) spectroscopic results (Qin *et al.* 2014).

Eucalyptus is widely used in the global plantation timber industry (Merkle and Nairn 2005). In the current study, eucalyptus fiber was pretreated by SESE. Scanning electron microscopy (SEM) and Van Soest fiber analysis were used to evaluate the effects of increased numbers of SESE pretreatment cycles on the structure and chemical composition of the eucalyptus fiber. The crystallinities of the pretreated materials were investigated by X-ray diffraction (XRD). Changes in the linkages and molecular weight distributions of lignin were characterized by ^{13}C NMR spectroscopy and gel permeation chromatography (GPC). Changes in the thermostability of lignin were evaluated by thermogravimetric analyses (TGA). The results are discussed in terms of structural differences, to determine how the SESE pretreatment intensity affects the structure.

EXPERIMENTAL

Materials

Eucalyptus was used as the raw material and was purchased from Guangdong Dingfeng Paper Co., Ltd. (Zhaoqing, Guangdong, P. R. China). The eucalyptus was ground and screened through a 10-mm mesh. Tap water (pH 7.5) was added to achieve a moisture content of 50 wt.%, and the resulting mixtures were sealed in plastic bags for 24 h at room temperature. Ethanol and phosphoric acid (H_3PO_4) were purchased from Sinopharm Chemical Reagents (Shanghai, P. R. China) and were used as received without further purification.

Screw extrusion steam explosion pretreatment

The continuous steam explosion apparatus consists of a feeding device, screw, barrel, die, electric motor, and gearbox (Ma *et al.* 2016). Eucalyptus fiber with a moisture content of 50% was fed into the barrel *via* a conveyor belt. The material was conveyed forward and compressed by continuous rotation of the meshing counter rotating tri-screw. Three screws were horizontally arranged. The adjacent screw had the opposite rotation, while other geometrical parameters were the same. The screw was divided into meshing and non-meshing areas according to the decreasing pitch of the three screws. The friction and shearing action between the eucalyptus fiber, barrel, and screw produced heat that vaporized water in the fiber. When the fiber reached the die outlet, the temperature and pressure of the material were 150 °C and 1.5 MPa, respectively. The fiber was rapidly discharged from the die, with a slit width of 1 mm. The duration of time with eucalyptus in the screw extrusion steam explosion apparatus was 15 s. The sudden pressure release destroyed the hierarchical structure of the eucalyptus fiber bundles. The intensity of the eucalyptus fiber pretreatment was adjusted by increasing the number of SESE cycles from one to four. Prior to the subsequent SESE cycle, a sample was removed and the moisture content of the remaining material was adjusted to 50 wt.% to offset evaporation occurring during SESE. The SESE apparatus, in contrast to conventional batch-type steam explosion that pretreats a set quantity of material at a time, can continuously process a large volume of material. Pretreated eucalyptus fiber samples are hereafter referred to as SESE-1, SESE-2, SESE-3, and SESE-4, with the suffix indicating the number of SESE cycles.

Preparation of lignin samples

Lignin samples were isolated according to a reported procedure (Zhang *et al.* 2007). Prior to oven drying for 6 h, eucalyptus fiber was dewaxed in 2:1 toluene:ethanol (v/v) for

24 h. Then, 5.0 g of air-dried eucalyptus fiber and 60 mL of phosphoric acid were loaded into a 200-mL glass beaker, heated to 50 °C, and stirred for 1 h. Next, 150 mL of 4:1 ethanol:deionized water (v/v) was added, and the resulting mixture was stirred in an ice water bath. After 15 min, the mixture was filtered. The filtration cake was rinsed with 4:1 ethanol:deionized water (v/v) until the filtrate became colorless. The combined filtrates were concentrated at 60 °C under reduced pressure to recycle the ethanol. Deionized water of three times the volume of the concentrated liquid was added. The mixture was centrifuged to separate the lignin. The solid residue was rinsed with deionized water until the filtrate was neutral, after which the solid residue was dried at 60 °C. Lignin samples are hereafter referred to as RAW-L (raw material), PE-L1, PE-L2, PE-L3, and PE-L4, with the suffix indicating the number of SESE cycles.

Methods

The chemical compositions of the raw and pretreated eucalyptus fibers were determined according to the Van Soest fiber detergent system (Fibretherm FT12, Gerhard, Germany). The procedure was performed as previously reported (Van Soest *et al.* 1991). This analysis provides the weight fraction of neutral detergent soluble, hemicelluloses (acid detergent soluble), cellulose (sulfuric acid hydrolysis soluble), and lignin (acid detergent lignin) contained in eucalyptus samples. All Van Soest fiber analyses were performed in triplicate, and the results are presented as averages of these three analyses.

A SEM (LEO1530VP, Zeiss, Germany) was used to evaluate the surface morphology of the fibers. The effect of different intensity pretreatments was assessed by comparing SEM images of the raw material to those of pretreated materials (SESE-1, SESE-2, SESE-3, and SESE-4). The SEM samples were placed on an aluminum stub and incubated in an oven at 60 °C. Prior to analysis, the powder samples were placed on specimen holders using double-sided conductive adhesive tape and were coated with gold to produce a 10-mm-thick film on the sample surface. The SEM accelerating voltage was fixed at 5 kV.

An XRD device was used to investigate the crystallinities of the eucalyptus fibers after different pretreatment intensities. Each sample in the form of milled powder was placed on the sample holder and levelled to obtain total and uniform X-ray exposure. The samples were examined using an X-ray diffractometer (Bruker D8-Advance, Madison, WI USA) at room temperature with monochromatic Cu Kα radiation (λ = 0.154 nm) in step-scan mode at 2θ ranging from 5° to 40° with a step size of 0.04° and a scanning speed of 0.2 s per step. The crystallinity index (CrI) was determined based on a conventional method (Segal *et al.* 1959). The crystallinity index (CI) was calculated from the ratio of the intensity of the 200 peak (I_{002}, 2θ = 22.5°) to the intensity of the minimum between the 200 and 110 peaks (I_{am}, 2θ = 18°), using Eq. (1) (Segal *et al.* 1959):

$$CI = (I_{002} - I_{am}) / I_{002} \times 100\% \quad (1)$$

where I_{002} contains contributions from both the crystalline and amorphous materials, and I_{am} contains only the amorphous contribution.

To investigate the structures of lignin isolated from the raw and pretreated fibers, the solid-state ^{13}C NMR spectra of lignin samples were recorded using a AVIII 400 MHz spectrometer (Bruker, Madison, WI, USA) with a frequency of 100.6 MHz, 50 ms acquisition time, 8 ms contact time, and 5 s repetition time. The sample was placed in a 4-mm-diameter ZrO_2 rotor. Spectra were recorded under a combination of cross-polarization, high-power proton decoupling, and magic angle spinning.

The thermal stability of the isolated lignin was evaluated by TGA using a Mettler Toledo thermo-gravimetric analyzer (TGA/SDTA 85-F, Zurich, Switzerland). An amount of 10 mg of sample was used for each measurement. All of the measurements were performed under a nitrogen atmosphere with a gas flow rate of 10 mL min^{-1}. The samples were heated from room temperature to 900 °C at a heating rate of 10 °C min^{-1}. The analyses were performed in triplicate.

The number-average molecular weight ($\overline{M_n}$) and weight-average molecular weight ($\overline{M_w}$) of isolated lignin were determined by GPC (Agilent 1100 HPLC system, Santa Clara, CA, USA), equipped with an ultraviolet detector. High performance liquid chromatography (HPLC)-grade tetrahydrofuran was used as the eluent at a flow rate of 1 mL min^{-1}. All of the lignin samples were acetylated according to a reported procedure before analysis (Wen *et al.* 2013a). A 4-mg sample of acetylated lignin was dissolved in 4 mL of tetrahydrofuran and 20 μL of the resulting solution was injected for GPC analysis.

RESULTS AND DISCUSSION

Eucalyptus Fiber Composition

Losses in weight at each process step were defined as neutral detergent soluble (NDS), acid detergent soluble (ADS), sulfuric acid hydrolysis soluble (SHS), or acid detergent lignin (ADL), according to the Van Soest fiber analysis method (Peltre *et al.* 2010).

The chemical compositions of eucalyptus fibers after different numbers of SESE cycles are shown in Table 1. Eucalyptus is a hardwood with a compact and dense structure, so a high pretreatment intensity was required to disrupt its structure. The acid detergent removed degraded carbohydrate products (Jacquet *et al.* 2011). Cellulose in the eucalyptus fiber was degraded during SESE, and these degradation fractions were removed during the acid washing process. More cellulose was degraded with increased numbers of SESE cycles. As a result, the SHS content decreased and the ADS content increased with increased numbers of SESE cycles. The increase in ADS content was small because hemicellulose also degraded. The NDS fraction of eucalyptus fiber corresponds to proteins, fats, and partial hydrolysates formed from the exposure of carbohydrates to acetic and other organic acids (formed from acetyl and other functional groups) (Jacquet *et al.* 2011). The product that resulted from the degradation of hemicellulose during SESE pretreatment was water-soluble and was removed in the NDS process. The hydrolysis of hemicellulose, and therefore the NDS content, increased with increased numbers of SESE cycles. The Duncan test was used to compare the results between different pretreatment cycles. The SHS content decreased, and the NDS and ADS contents increased with increasing number of pretreatment cycles. This was consistent with the degradation of hemicellulose and cellulose.

The analysis of variance (Table 1) revealed that all pretreated materials had significantly lower means for SHS contents, and higher means for NDS and ADS contents, when compared to the raw materials. The SESE-4 sample had the lowest mean for SHS content and highest mean for NDS and ADS contents. The compositions differed significantly with different numbers of pretreatment cycles.

Table 1. Chemical Compositions of Eucalyptus Fibers after Increasing Numbers of SESE Pretreatment Cycles

Composition (%w/w)	NDS	ADS	SHS	ADL
Raw Material	7.66±0.42^{d}	12.69±0.57^{d}	52.52±0.74^{a}	22.07±0.57^{d}
SESE-1	8.72±0.39^{c}	13.87±0.40^{c}	47.13±0.55^{b}	22.66±0.85^{c}
SESE-2	9.33±0.21^{b}	14.01±0.82^{c}	46.83±0.61^{c}	23.83±0.50^{a}
SESE-3	9.24±0.48^{b}	15.52±0.12^{b}	45.23±0.69^{c}	23.8±0.27^{a}
SESE-4	10.37±0.64^{a}	16.4±0.33^{a}	43.59±0.81^{d}	23.15±0.31^{b}

$^{a-d}$ Means in the same column having different superscript letters are significantly different at 5% probability.

Crystallinity of Eucalyptus Fiber

The effect of SESE pretreatment on the crystallinity of eucalyptus fiber is shown in Fig. 1 and Table 2. The XRD peaks were observed at around 16.6° and 22.7° 2θ in the patterns of all samples, indicating that the structure of cellulose remained as cellulose-I after SESE pretreatment (Sugiyama *et al.* 1991). The intensity of the diffraction peak, related to the crystallinity of eucalyptus fiber, changed slightly after SESE pretreatment. The SESE resulted in a lower crystallinity of pretreated samples compared to the raw material (42.2%). Amorphous regions were damaged during SESE, which acted to increase the crystallinity. The SESE also disrupted the crystalline regions of cellulose, which acted to decrease the crystallinity (Park *et al.* 2010). The latter factor is dominant, so a slight decrease in crystallinity was observed with increasing numbers of SESE cycles.

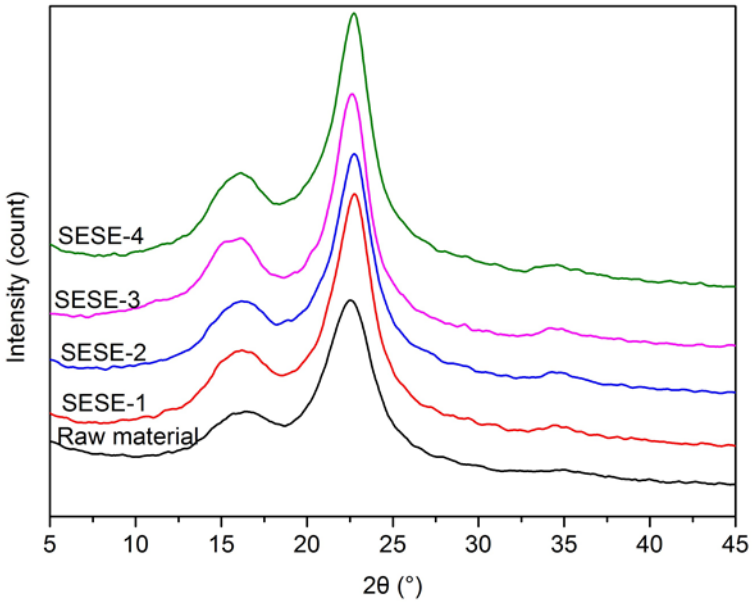

Fig. 1. XRD patterns of eucalyptus fibers after increasing numbers of SESE pretreatment cycles

Table 2. Crystallinity of Eucalyptus Fibers after Increasing Numbers of SESE Pretreatment Cycles

Sample	Crystallinity (%)
Raw Material	42.2
SESE-1	38.0
SESE-2	39.1
SESE-3	40.0
SESE-4	37.1

Morphology of Eucalyptus Fiber

The SEM images of the micron-scale morphology of raw and SESE pretreated samples are shown in Fig. 2. Figure 2a shows that eucalyptus fiber bundles in the raw material were arranged in neat rows and Fig. 2b shows that these bundles had smooth surfaces. After one SESE pretreatment cycle (Fig. 2c), the radial size of the fiber bundles decreased noticeably and the arrangement of the fiber bundles was damaged by the mechanical action of the SESE process. Partial fibers were stripped out of the bundles. The high magnification SEM image in Fig. 2d shows that the surface became roughened and that damage to the fiber surface was not uniform. The molecular structures of the plant cell walls consist of a laminated structure (middle lamella, primary cell wall, and secondary cell wall) and fibers of different layers oriented in different directions (Kirby 2011). In this study, the fiber size decreased from hundreds to several micrometers with increasing numbers of SESE pretreatment cycles. Microfibrils were apparent in the SEM images of the pretreated fibers (Figs. 2d, 2f, 2g, 2h, and 2j). The microfibril angles observed in Figs. 2d and 2f were > 30°, which indicated that these microfibrils contributed to the outermost layer of the secondary wall (S1). Further SESE pretreatment resulted in microfibril angles of approximately 20° (Figs. 2h and 2j). This indicates that the middle lamella, primary wall, and S1 layer were removed, exposing the middle layer of the secondary wall (S2) (Ma *et al.* 2016). Figure 2h shows that the S1 layer was partially removed after three SESE pretreatment cycles. Figure 2j shows that the S1 layer was almost completely removed after four SESE pretreatment cycles.

Structural Analysis of Eucalyptus Lignin

To further investigate the structures of the isolated lignins, the ^{13}C NMR spectra are shown in Fig. 3. Peaks were assigned according to previously-reported studies. The peak at 172.7 ppm was assigned to the C=O of aliphatic carboxyl groups (Wen *et al.* 2013b). Peaks at 152.4 ppm and 104.3 ppm were assigned to etherified syringyl units (C-3/C-5; C-2/C-6).

The low intensities of the peaks of the etherified syringyl units were caused by the cleavage of β-O-4 linkages during SESE (Wang *et al.* 2017). Peaks at 146.64 (C-4 etherified) ppm and 114.7 (C-2) ppm were assigned to guaiacyl units. These peaks collectively confirmed that the isolated lignin from eucalyptus was guaiacyl-syringyl (G-S)-enriched lignin.

Increasing the number of SESE pretreatment cycles to three resulted in a decrease in the intensity of the peaks (Asikkala *et al.* 2012) of aromatic C-C (δ140.0–123.0 ppm) and a decrease in the intensities of peaks of aromatic C-H (δ123.0–103.0 ppm). This phenomenon was explained by the condensation reaction that occurs during SESE that

could have resulted in the replacement of C-H bonds with C-C bonds. The intensity of the peak at δ140.0–123.0 ppm decreased and the intensity of the peak at δ123.0–103.0 ppm increased after three SESE pretreatment cycles. This indicated that the degree of condensation did not increase indefinitely. The peaks at 73.9 ppm (C-1, xylan) showed that xylan was present in all samples, which indicated that the isolation process was incomplete. This result indicated that xylan was covalently bound to the lignin, and this finding was consistent with previous reports.

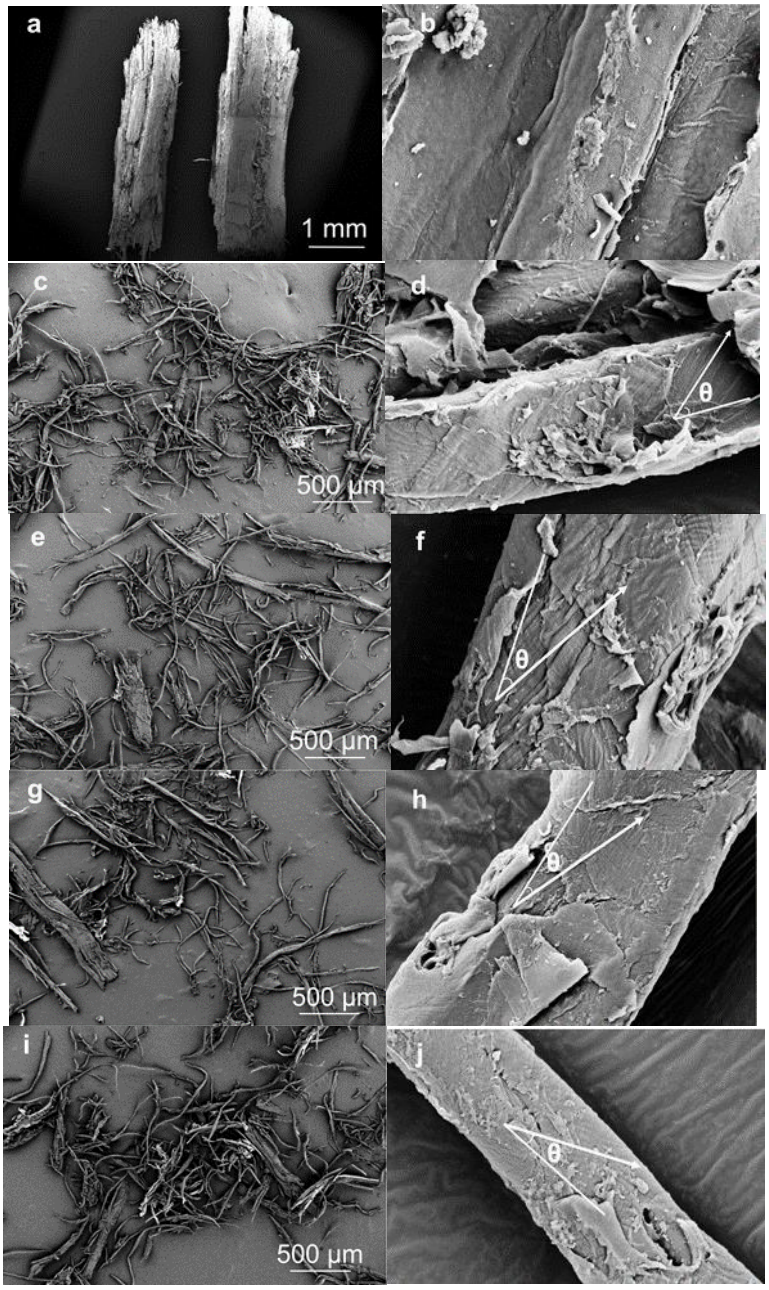

Fig. 2. SEM images of (a)/(b) raw material, (c)/(d) SESE-1, (e)/(f) SESE-2, (g)/(h) SESE-3, and (i)/(j) SESE-4; images in (b), (d), (f), and (h) were obtained at 5000× magnification

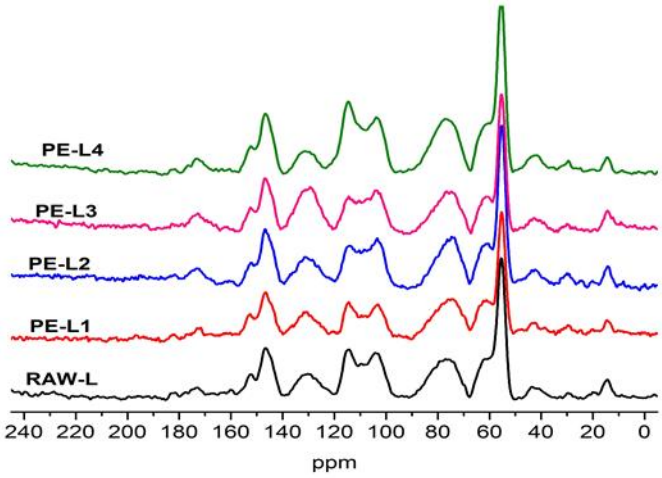

Fig. 3. ^{13}C NMR spectra of eucalyptus lignin after increasing numbers of SESE pretreatment cycles

The Yield of Lignin

Eucalyptus was subjected to SESE pretreatment to investigate the structural changes of lignin during the SESE process. Lignin isolated from eucalyptus was used as a reference. Table 3 shows that the yield of lignin was 25.51%, 34.16%, 37.29%, 39.72%, and 40.64% for Raw-L, PE-L1, PE-L2, PE-L3, and PE-L4, respectively. The increasing yield suggested that SESE pretreatment facilitated the extraction of lignin from eucalyptus. This conclusion is consistent with Suzuki *et al*. (1998), who reported that lignin on the fiber substrate surface was readily extracted during SE. The increasing lignin yield with increasing number of SESE pretreatment cycles could be explained as follows. The pretreated material was strongly disrupted, decreasing the fiber size from hundreds of micrometers to several micrometers, which facilitated the extraction of lignin. Some lignin in the pretreated eucalyptus also became depolymerized and fragmented during the SESE process, which promoted lignin dissolution in the subsequent extraction process. The growth rate of yield became more moderate with increasing number of SESE pretreatment cycles. It was concluded that the condensation of lignin inhibited its extraction. GPC results showed that lignin condensation was more significant with increasing number of SESE pretreatment cycles.

Molecular Weight Analysis of Eucalyptus Lignin

The molecular weights of the isolated lignin are shown in Fig. 4. The lignin molecular weight distribution curve of the raw material was bimodal. This indicates that the eucalyptus lignin contained two fractions with differing molecular weights. The SESE pretreatment caused the lignin molecular weight distribution curve to become multimodal. Specifically, the molecular weight distribution became wider and the peak position changed. This change in molecular weight arose from the eucalyptus fiber undergoing dynamic physicochemical and mechanical action during SESE, which destroyed the lignin structure and formed lignin fragments. The degradation of lignin was accompanied by comprehensive condensation. Competing degradation and condensation reactions led to the generation of lower molecular weight lignin ($< 10^3$ g mol^{-1}) and higher molecular weight lignin ($> 6 \times 10^4$ g mol^{-1}), and thus a more heterogeneous lignin structure. The

results revealed that the more heterogeneous lignin structure after SESE pretreatment led to an increase in polydispersity. Table 3 shows that the polydispersity of pretreated lignin increased to 3.99, compared to 2.45 for raw lignin.

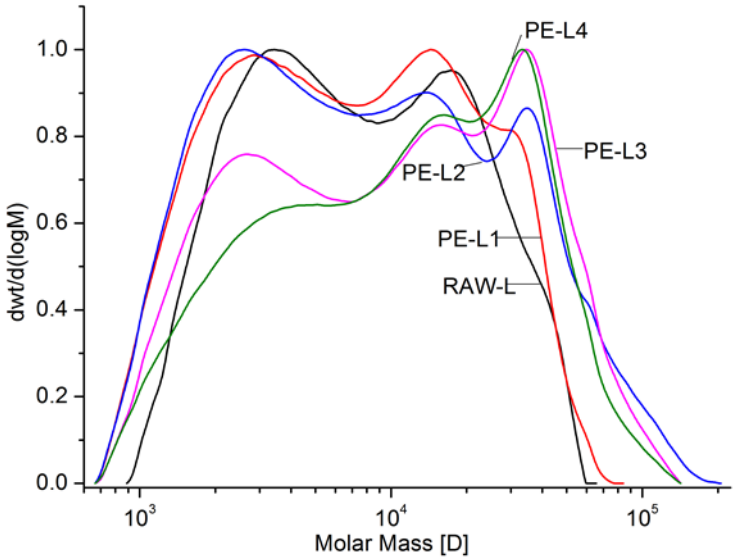

Fig. 4. Molecular weight distribution of eucalyptus lignin after increasing numbers of SESE pretreatment cycles

Table 3. Number-average Molecular Weight (M_n), Weight-average Molecular Weight (M_w), Polydispersity (M_w/M_n) and Yield of Lignin Isolated from Eucalyptus Fiber

Sample	M_n (g mol^{-1})	M_w (g mol^{-1})	Polydispersity	Yield[a] (%)
Raw-L	3560	8727	2.45	25.51
PE-L1	3986	11650	2.92	34.16
PE-L2	4215	16760	3.98	37.29
PE-L3	4860	18580	3.82	39.72
PE-L4	5343	18400	3.44	40.64

[a] The yield was calculated based on the klason lignin in Eucalyptus.

The observed lignin molecular weight of < 10^3 g mol^{-1} could be rationalized by the formation of small lignin fragments from lignin degradation (Sun *et al.* 2000). Lignin fragments generated during pretreatment have been shown to repolymerize by acid-catalyzed condensation between aromatic C6 or C5 moieties and carbonium ions (El Hage *et al.* 2010). Figure 4 shows that a peak at 4 × 10^4 g mol^{-1} and the lignin molecular weight of < 10^3 g mol^{-1} were observed after SESE pretreatment. The higher-molecular-weight peak indicated condensation during SESE. The content of lignin with molecular weights of 7 × 10^3 g mol^{-1} to 9 × 10^4 g mol^{-1} decreased with increased numbers of SESE pretreatment cycles. The peak related to higher molecular weights of 3 g mol^{-1} × 10^4 g mol^{-1} to 2 × 10^5 g mol^{-1} increased with increasing numbers of SESE pretreatment cycles, which indicated an increasing degree of lignin condensation. Table 3 shows that the M_w increased from 8727 g mol^{-1} to 18400 g mol^{-1}. The M_n also increased from 3560 g mol^{-1} to 5343 g mol^{-1} with increasing number of SESE pretreatment cycles. This indicated that

condensation became progressively more important with increasing number of pretreatment cycles. After three cycles, the molecular weight distribution and peak position of the lignin stabilized. Lignin simultaneously became degraded, which also decreased its molecular weight after SESE pretreatment. The molecular weight and distribution of lignin therefore did not increase indefinitely with increasing numbers of SESE pretreatment cycles.

Thermal Stability of Eucalyptus Lignin

Figures 5a and 5b show the TG and DTG curves of eucalyptus lignin after increasing numbers of SESE pretreatment cycles, respectively. The thermal decomposition of lignin is related to its structure and functional groups. The weight loss at 300 °C to 400 °C was attributed to the cleavage of ether linkages and oxidation of lignin side chains (*i.e.* carboxylation/carbonylation of aliphatic hydroxyl groups, side chain dehydrogenation) (Fenner and Lephardt 1981; Sun *et al.* 2000). The maximum thermal decomposition temperature (DTG_{max}) was used to evaluate the thermal stabilities of the lignin samples. The DTG_{max} values were 352.4 °C, 355.8 °C, 357.8 °C, 358.4 °C, and 357.2 °C for RAW-L, PE-L1, PE-L2, PE-L3, and PE-L4, respectively. Comparing to RAW-L, the DTG_{max} of PE-L shifted to higher temperature, indicating a more stable lignin structure (Wen *et al.* 2013a). For the aromatic structure of lignin, a higher degree of condensation reportedly results in a more stable structure. The relatively stable lignin structure was caused by condensation, as evidenced by ^{13}C NMR observations (Tejado *et al.* 2007; Wen *et al.* 2013a). The small weight loss peak at 200 °C to 300 °C in the DTG curve was related to the degradation of carbohydrates, and it showed that a part of degradation of carbohydrates was connected with the isolated lignin. This conclusion was consistent with the ^{13}C NMR observations of xylan covalently bound to lignin. The weight loss at 400 °C to 600 °C was predominantly related to the degradation and condensation of the aromatic ring of lignin (Sun *et al.* 2000). The DTG peak at > 400 °C in PE-L corresponded to higher molecular weight lignin, which can be observed in Fig. 4. Thus, thermal stability of lignin increased, and the maximum rate of weight loss (DTG_{max}) decreased after SESE pretreatment.

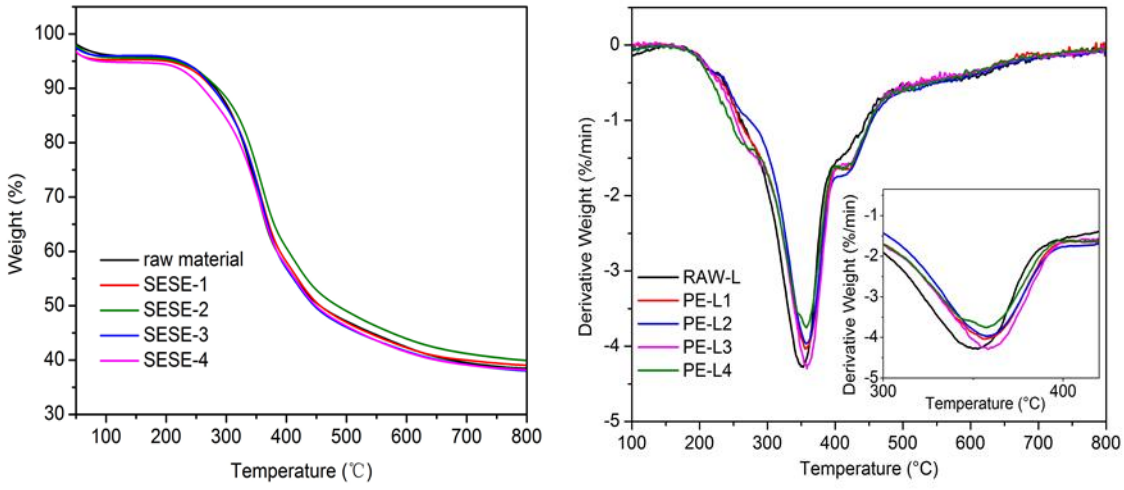

(a) (b)

Fig. 5. (a) TG and (b) DTG curves of eucalyptus lignin after increasing numbers of SESE pretreatment cycles

CONCLUSIONS

1. The analyses of chemical compositions indicated that hemicellulose and cellulose were effectively degraded and removed from eucalyptus fiber *via* screw extrusion steam explosion (SESE) pretreatment.
2. The crystal structure of cellulose was destroyed and crystallinity decreased during the SESE pretreatment. The SESE also damaged the surface and decreased the size of the eucalyptus fiber bundles.
3. The ^{13}C NMR indicated that the isolated lignin was typical G-S-enriched lignin of hardwood. The SESE pretreatment led to the simultaneous cleavage of linkages and condensation of lignin.
4. The increased molecular weight of SESE-pretreated eucalyptus lignin showed that the condensation of lignin played a dominant role. The thermostability of lignin increased with SESE pretreatment up to three cycles, and then it remained stable with further SESE pretreatment, which corresponded to the observed trend in its molecular weight.
5. These findings demonstrated that SESE pretreatment destroyed the tissue structure and initially separated components of the eucalyptus fiber, and that SESE could achieve a similar result to conventional batch-type SE. However, the SESE pretreatment of lignocellulose was more efficient and realized continuous production, and thus is more suitable for industrial application.

ACKNOWLEDGMENTS

The authors acknowledge financial support from The National Natural Science Foundation of China (No. 51373058), the Science and Technology Planning Project of Guangdong Province, P.R. China (No. 2014B090921006), and the Special Support Program of Guangdong Province (No. 2015TX01X151), the Special-funded Program on National Key Scientific Instruments and Equipment Development of China (Grant No. 2012YQ23004305), and the Science and Technology Planning Project of the Department of Science and Technology of Guangdong Province, P. R. China (No. 2015B090904004).

REFERENCES CITED

Asikkala, J., Tamminen, T., and Argyropoulos, D. S. (2012). "Accurate and reproducible determination of lignin molar mass by acetobromination," *Journal of Agricultural and Food Chemistry* 60(36), 8968-8973. DOI: 10.1021/jf303003d

El Hage, R., Brosse, N., Sannigrahi, P., and Ragauskas, A. (2010). "Effects of process severity on the chemical structure of miscanthus ethanol organosolv lignin," *Polymer Degradation and Stability* 95(6), 997-1003. DOI: 10.1016/j.polymdegradstab.2010.03.012

Fang, H., Deng, J., and Zhang, T. (2011a). "Dilute acid pretreatment of black spruce using continuous steam explosion system," *Applied Biochemistry and Biotechnology* 163(4), 547-557. DOI: 10.1007/s12010-010-9061-6

Fang, H., Deng, J., and Zhang, X. (2011b). "Continuous steam explosion of wheat straw by high pressure mechanical refining system to produce sugars for bioconversion," *BioResources* 6(4), 4468-4480. DOI: 10.15376/biores.6.4.4468-4480

Feng, Y., Lei, B., Liang, Y., Zhong, H., Yin, X., Qu, J., and He, H. (2016). "Changes in the microstructure and components of *Eulaliopsis binata* treated by continuous screw extrusion steam explosion," *BioResources* 11(4), 9455-9466. DOI: 10.15376/biores.11.4.9455-9466

Fenner, R. A., and Lephardt, J. O. (1981). "Examination of the thermal decomposition of kraft pine lignin by Fourier transform infrared evolved gas analysis," *Journal of Agricultural and Food Chemistry* 29(4), 846-849. DOI: 10.1021/jf00106a042

Inoue, H., Yano, S., Endo, T., Sakaki, T., and Sawayama, S. (2008). "Combining hot-compressed water and ball milling pretreatments to improve the efficiency of the enzymatic hydrolysis of eucalyptus," *Biotechnology for Biofuels* 1(1), 2. DOI: 10.1186/1754-6834-1-2

Jacquet, N., Quievy, N., Vanderghem, C., Janas, S., Blecker, C., Wathelet, B., and Paquot, M. (2011). "Influence of steam explosion on the thermal stability of cellulose fibres," *Polymer Degradation and Stability* 96(9), 1582-1588. DOI: 10.1016/j.polymdegradstab.2011.05.021

Karimi, K., and Taherzadeh, M. J. (2016). "A critical review on analysis in pretreatment of lignocelluloses: Degree of polymerization, adsorption/desorption, and accessibility," *Bioresource Technology* 203, 348-356. DOI: 10.1016/j.biortech.2015.12.035

Kirby, A. R. (2011). "Atomic force microscopy of plant cell walls," *The Plant Cell Wall: Methods and Protocols* 715, 169-178. DOI: 10.1007/978-1-61779-008-9_12

Ma, P., Lan, J., Feng, Y., Liu, R., Qu, J., and He, H. (2015). "Effects of continuous steam explosion on the microstructure and properties of eucalyptus fibers," *BioResources* 11(1), 1417-1431. DOI: 10.15376/biores.11.1.1417-1431

Meng, X., and Ragauskas, A. J. (2014). "Recent advances in understanding the role of cellulose accessibility in enzymatic hydrolysis of lignocellulosic substrates," *Current Opinion in Biotechnology* 27, 150-158. DOI: 10.1016/j.copbio.2014.01.014

Merkle, S. A., and Nairn, C. J. (2005). "Hardwood tree biotechnology," *In Vitro Cellular and Developmental Biology-Plant* 41(5), 602-619. DOI: 10.1079/IVP2005687

Park, S., Baker, J. O., Himmel, M. E., Parilla, P. A., and Johnson, D. K. (2010). "Cellulose crystallinity index: Measurement techniques and their impact on interpreting cellulase performance," *Biotechnology for Biofuels* 3(1), 10. DOI: 10.1186/1754-6834-3-10

Peltre, C., Dignac, M. F., Derenne, S., and Houot, S. (2010). "Change of the chemical composition and biodegradability of the Van Soest soluble fraction during composting: A study using a novel extraction method," *Waste Management* 30(12), 2448-2460. DOI: 10.1016/j.wasman.2010.06.021

Pu, Y., Hu, F., Huang, F., Davison, B. H., and Ragauskas, A. J. (2013). "Assessing the molecular structure basis for biomass recalcitrance during dilute acid and hydrothermal pretreatments," *Biotechnology for Biofuels* 6(1), 15. DOI: 10.1186/1754-6834-6-15

Qin, W., Zheng, Z. M., Kang, P., Dong, C., and Yang, Y. (2014). "Solution-sensitivity and comprehensive mechanism of lignin breakdown during the phosphoric acid-acetone pretreatment process," *BioResources* 9(1), 628-641.

Segal, L. G. J. M. A., Creely, J. J., Martin Jr, A. E., and Conrad, C. M. (1959). "An empirical method for estimating the degree of crystallinity of native cellulose using the X-ray diffractometer," *Textile Research Journal* 29(10), 786-794. DOI: 10.1177/004051755902901003

Sugiyama, J., Persson, J., and Chanzy, H. (1991). "Combined infrared and electron diffraction study of the polymorphism of native celluloses," *Macromolecules* 24(9), 2461-2466. DOI: 10.1021/ma00009a050

Sun, R., Tomkinson, J., and Jones, G. L. (2000). "Fractional characterization of ash-AQ lignin by successive extraction with organic solvents from oil palm EFB fibre," *Polymer Degradation and Stability* 68(1), 111-119. DOI: 10.1016/S0141-3910(99)00174-3

Suzuki, S., Shintani, H., Seungyoung, P., Saito, K., Laemsak, N., and Okuma, M. (1998). "Preparation of binderless boards from steam exploded pulps of oil palm (*Elaeis guneensis* Jacq.) fronds and structural characteristics of lignin and wall polysaccharides in steam exploded pulps to be discussed for self-bindings," *Holzforschung - International Journal of the Biology, Chemistry, Physics and Technology of Wood* 52(4), 417-426. DOI: 10.1515/hfsg.1998.52.4.417

Tejado, A., Pena, C., Labidi, J., Echeverria, J. M., and Mondragon, I. (2007). "Physico-chemical characterization of lignins from different sources for use in phenol–formaldehyde resin synthesis," *Bioresource Technology* 98(8), 1655-1663. DOI: 10.1016/j.biortech.2006.05.042

Van Soest, P. V., Robertson, J. B., and Lewis, B. A. (1991). "Methods for dietary fiber, neutral detergent fiber, and nonstarch polysaccharides in relation to animal nutrition," *Journal of Dairy Science* 74(10), 3583-3597. DOI: 10.3168/jds.S0022-0302(91)78551-2

Wang, X., Guo, Y., Zhou, J., and Sun, G. (2017). "Structural changes of poplar wood lignin after supercritical pretreatment using carbon dioxide and ethanol–water as co-solvents," *RSC Advances* 7(14), 8314-8322. DOI: 10.1039/C6RA26122A

Wen, J. L., Xue, B. L., Sun, S. L., and Sun, R. C. (2013a). "Quantitative structural characterization and thermal properties of birch lignins after auto-catalyzed organosolv pretreatment and enzymatic hydrolysis," *Journal of Chemical Technology and Biotechnology* 88(9), 1663-1671. DOI: 10.1002/jctb.4017

Wen, J. L., Xue, B. L., Xu, F., Sun, R. C., and Pinkert, A. (2013b). "Unmasking the structural features and property of lignin from bamboo," *Industrial Crops and Products* 42, 332-343. DOI: 10.1016/j.indcrop.2012.05.041

Zhang, Y. H. P., Ding, S. Y., Mielenz, J. R., Cui, J. B., Elander, R. T., Laser, M., and Lynd, L. R. (2007). "Fractionating recalcitrant lignocellulose at modest reaction conditions," *Biotechnology and Bioengineering* 97(2), 214-223. DOI: 10.1002/bit.21386

Zhao, X., Zhang, L., and Liu, D. (2012). "Biomass recalcitrance. Part II: Fundamentals of different pre-treatments to increase the enzymatic digestibility of lignocellulose," *Biofuels, Bioproducts and Biorefining* 6(5), 561-579. DOI: 10.1002/bbb.1350

Article submitted: July 10, 2017; Peer review completed: September 10, 2017; Revised version received and accepted: January 21, 2018; Published: February 1, 2018.
DOI: 10.15376/biores.13.2.2204-2217